Efficient Inverse Scattering Algorithm by Incorporating RPM Method for Microwave Non-destructive Imaging

Shuto Takahashi
Graduate School of Informatics and Engineering,
University of Electro-Communications,
Tokyo, Japan
takahashi.shuto@ems.cei.uec.ac.jp

Shouhei Kidera
Graduate School of Informatics and Engineering,
University of Electro-Communications,
Tokyo, Japan
Japan Science Technology Agency, PRESTO,
Saitama, Japan
kidera@ee.uec.ac.jp

***Abstract*—Microwave non-destructive testing (NDT) is promising for detection of an air cavity or a metallic corrosion buried into concrete road or tunnel. The distorted born iterative method (DBIM) is one of the most effective approaches to reconstruct dielectric map and recognize a high contrast object. However, in an actual NDT observation model, it must be assumed that only reflection field is available, which makes the ill-posed problem extremely difficult. To solve this problem, the range points migration (RPM) based object area extraction scheme is incorporated into the DBIM, where the area of region of interest (ROI) is considerably downsized to reduce the number of unknowns in the DBIM. The finite-difference time-domain (FDTD) based numerical simulation tests demonstrate that our proposed method effectively enhance the accuracy of dielectric map reconstruction for the sparsely distributed object model.**

***Index Terms*—Inverse scattering analysis, Non-destructive testing (NDT), Distorted born iterative method (DBIM), Range points migration(RPM)**

I. Introduction

Microwave non-destructive testing (NDT) techniques have a great potential to achieve both deep penetration depth and retrieving dielectric property for the targeted object [1]. Microwave NDT is more suitable for large scale inspection compared with ultrasonic testing and hammering test because they basically require contact measurement to avoid a large propagation loss in the air. There is an emergent demand of detection of air cavity or metallic rust for aging transportation infrastructures such as tunnel or road, to avoid a voluntary collapse or catastrophe caused by an earthquake.

Various microwave imaging techniques has been proposed and they are mainly divided into the two categories. One is a confocal (radar) approach, most of which are based on delay and sum (DAS) algorithm, or synthetic aperture processing [2]. The other is an inverse scattering analysis [3], which can directly reconstruct dielectric profile by solving the Helmholtz type domain integral equation, but it is non-linear problem and often has an ill-posed property. In addition, in the typical NDT observation model, the tomographic observation model is not available, and an equivalent aperture size is considerably limited compared with that assumed in most of inverse scattering approaches.

However, the literature [4] reveals that there are significant difference among the types of metallic rust, e.g. red rust, black rust or salt rust, and the dielectric feature extraction is much promising for discrimination of erosion or air crack. As one of the most promising inverse scattering methods, adopts the distorted born iterative method (DBIM) [5], which has been demonstrated that it accurately reconstructs dielectric profile for the target with high dielectric contrast compared with that of the background media. However, a reflected electric field is only available in non-destructive testing, which causes lack of information and makes estimation difficult. Also, to investigate large scale are with high resolution, a large number of unknown quantities must be estimated, which incurs high computational cost and deterioration of reconstructed profile.

Thus, to alleviate the ill-posedness in inverse scattering approach, this paper proposes the incorporation of radar approach and inverse scattering approach, where the region of interest (ROI) in inverse scattering is considerably downsized by radar imaging results. In particular, this paper focuses on the RPM method to determine the ROI area before the DBIM process, the effectiveness of which has been demonstrated in number of literature [6], [7]. For the NDT application, the study [8] revealed that the RPM achieves that 1/100 wavelength accuracy for target boundary extraction inside of concrete media, with considerably lower computational cost in comparison with delay-and-sum (DAS) based algorithm. By determining the ROI area by RPM, the number of unknowns processed in DBIM are considerably downsized, which contribute to offer accurate reconstruction of dielectric profile of targets, even in a seriously ill-posed situation. The FDTD-based numerical simulation, assuming the typical NDT scenario with air cavity or some types of metallic rusts, demonstrates that the proposed algorithm considerably enhances the reconstruction accuracy and the convergence speed, compared with the original DBIM.

ISBN 978-90-827970-1-5

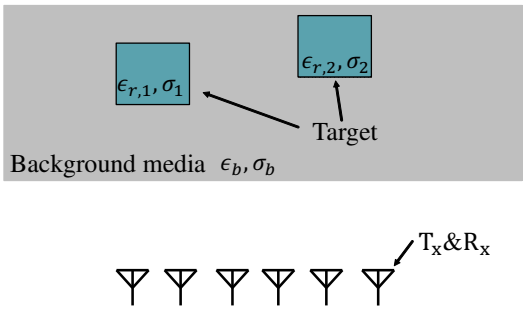

Fig. 1: Observation model.

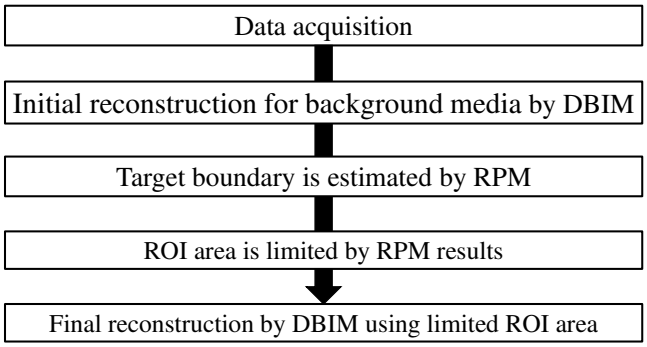

Fig. 2: Flowchart of the proposed method.

II. System model

Figure 1 shows the observation model. It assumes that a background media is homogeneous, low lossy, and non-dispersive dielectric media. A number of the transmitting and receiving antennae are arranged in front of background media. Note that, the relative permittivity and conductivity of background media are not given. The filter output (*e.g.* matched filter) at antenna location $\boldsymbol{r}$ is defined as $E(\boldsymbol{r}, R)$, where $R = ct/2$ expressed by time t and c is the speed of light in air. Range points extracted from local maxima of $E(\boldsymbol{r}, R)$ as to R are divided into two groups. one is defined as $\boldsymbol{q}_{1,i} \equiv (\boldsymbol{r}_{1,i}, R_{1,i})$ where each member having maximum $E(\boldsymbol{r}, R)$ as to R. The remaining range points are categorized into $\boldsymbol{q}_{2,i} \equiv (\boldsymbol{r}_{2,i}, R_{2,i})$.

III. Proposed Method

A. Distorted Born Iterative method (DBIM)

The reconstruction problem for complex permittivity distribution using scattered field can be solved by the Helmholtz type integral equation, that is;

$$E^{\mathrm{s}}(\boldsymbol{r}, \omega) = \omega^2 \mu \int_{\Omega} G_0(\boldsymbol{r}', \boldsymbol{r}, \omega) E^{\mathrm{t}}(\boldsymbol{r}', \omega) O(\boldsymbol{r}') d\boldsymbol{r}', \quad (1)$$

where the Ω is region of interest (ROI) including targeted object, $E^{\mathrm{t}}(\boldsymbol{r}, \omega)$ is the total electric field. The scattered field is defined as $E^{\mathrm{s}}(\boldsymbol{r}, \omega) \equiv E^{\mathrm{t}}(\boldsymbol{r}, \omega) - E^{\mathrm{i}}(\boldsymbol{r}, \omega)$, where $E^{\mathrm{i}}(\boldsymbol{r}, \omega)$ is the incident electric field in the presence of the actual background complex relative permittivity denoted as $\epsilon_0(\boldsymbol{r})$. $G(\boldsymbol{r}', \boldsymbol{r}, \omega)$ is the Green's function and $O(\boldsymbol{r}) = \epsilon_r(\boldsymbol{r}) - \epsilon_b(\boldsymbol{r})$ is the object function where $\epsilon_r(\boldsymbol{r})$ is an actual complex relative permittivity of the scatters. The difference between observed total electric field and that obtained by assuming background complex relative permittivity $\epsilon_{\mathrm{b}}(\boldsymbol{r})$ is formulated as:

$$\begin{aligned} \Delta E^{\mathrm{t}}(\boldsymbol{r}, \omega) &= E^{\mathrm{t}}(\boldsymbol{r}, \omega) - E^{\mathrm{t}}_{\mathrm{b}}(\boldsymbol{r}, \omega) \\ &= \omega^2 \mu \int_{\Omega} G_{\mathrm{b}}(\boldsymbol{r}', \boldsymbol{r}, \omega) E^{\mathrm{t}}(\boldsymbol{r}', \omega) \Delta O(\boldsymbol{r}') d\boldsymbol{r}', \end{aligned} \quad (2)$$

where $G_{\mathrm{b}}(\boldsymbol{r}', \boldsymbol{r}, \omega)$ is the Green's function of the background medium, $\Delta O(\boldsymbol{r}) = O(\boldsymbol{r}) = \epsilon_r(\boldsymbol{r}) - \epsilon_{\mathrm{b}}(\boldsymbol{r})$. Here, assuming that $\Delta O(\boldsymbol{r})$ is sufficiently small, $E^{\mathrm{t}}(\boldsymbol{r}, \omega) \simeq E^{\mathrm{t}}_{\mathrm{b}}(\boldsymbol{r}, \omega)$ holds, and Eq. (2) is approximated as:

$$\Delta E^{\mathrm{t}}(\boldsymbol{r}, \omega) \simeq \omega^2 \mu \int_{\Omega} G_{\mathrm{b}}(\boldsymbol{r}', \boldsymbol{r}, \omega) E^{\mathrm{t}}_{\mathrm{b}}(\boldsymbol{r}', \omega) \Delta O(\boldsymbol{r}') d\boldsymbol{r}'. \quad (3)$$

The DBIM iteratively updates $\epsilon_b(\boldsymbol{r})$, $G_{\mathrm{b}}(\boldsymbol{r}', \boldsymbol{r}, \omega)$ and $E^{\mathrm{t}}_{\mathrm{b}}(\boldsymbol{r}, \omega)$ in order to minimize $|\Delta E^{\mathrm{t}}(\boldsymbol{r}, \omega)|^2$.

A number of study revealed that the DBIM offers accurate dielectric profiles even with high contrast object under tomographic observation model, however, in most case of NDT scenario, a tomographic observation could not be assumed, namely, quite narrower aperture size is available. Thus, it makes the ill-posed problem more difficult to obtain a meaningful solution.

B. Range Points Migration (RPM)

To overcome the above difficulty, this paper introduces the RPM-based ROI limitation to reduce the number of unknowns in the DBIM algorithm. Here, in typical NDT case, the targeted object, *e.g.* air cavity, metallic rust or other cracks is sparsely distributed in the homogeneous background media (i.e. concrete media). Under this assumption, the ROI area can be determined by the distribution of scattering centers, which can be accurately estimated by the RPM method [7]. At first, we briefly describe the principle of the RPM method as follows. RPM converts the range point $\boldsymbol{q}_{2,i}$ to the corresponding scattering center $\boldsymbol{p}(\boldsymbol{q}_{2,i})$ as:

$$\begin{aligned} \hat{\boldsymbol{p}}(\boldsymbol{q}_{2,i}) = \underset{\boldsymbol{p}^{\mathrm{int}}_{i,l,m}}{\arg\max} & \sum_{j,k} g(\boldsymbol{q}_{2,i}; \boldsymbol{q}_{2,j}, \boldsymbol{q}_{2,k}) \\ & \times \exp\left\{ -\frac{\|\boldsymbol{p}^{\mathrm{int}}_{i,j,k} - \boldsymbol{p}^{\mathrm{int}}_{i,l,m}\|^2}{\sigma_r^2} \right\}, \end{aligned} \quad (4)$$

where $\boldsymbol{p}^{\mathrm{int}}_{i,j,k}$ is the intersection point among the three orbits of propagation paths, usually determined by the dielec-

ISBN 978-90-827970-1-5 © EURASIP 2018

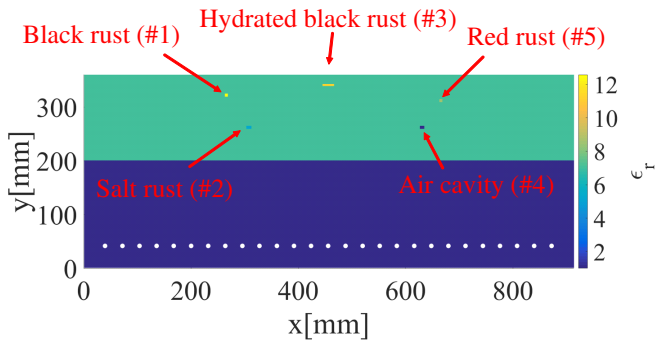

(a)

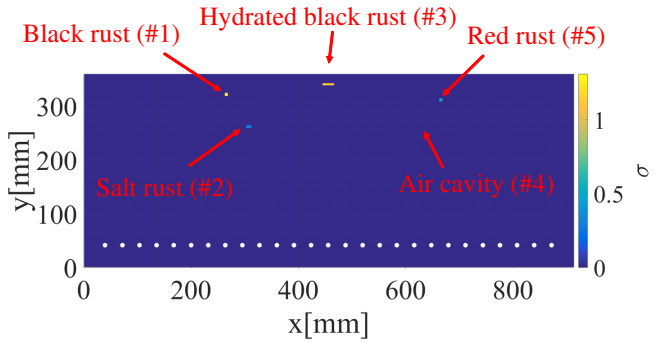

(b)

Fig. 3: Actual profile of (a) relative permittivity and (b) conductivity in numerical simulation model.

tric constant of the background media, σ_r is a constant. $g(\boldsymbol{q}_{2,i};\boldsymbol{q}_{2,j},\boldsymbol{q}_{2,k})$ is defined as:

$$g(\boldsymbol{q}_{2,i};\boldsymbol{q}_{2,j},\boldsymbol{q}_{2,k}) \equiv |s(\boldsymbol{q}_{2,j})|\exp\left\{-\frac{D^2_{XY,i,j}}{2\sigma^2_{XY}}-\frac{D^2_{Z,i,j}}{2\sigma^2_{Z}}-\frac{D^2_{R,i,j}}{2\sigma^2_{R}}\right\} + |s(\boldsymbol{q}_{2,k})|\exp\left\{-\frac{D^2_{XY,i,k}}{2\sigma^2_{XY}}-\frac{D^2_{Z,i,k}}{2\sigma^2_{Z}}-\frac{D^2_{R,i,k}}{2\sigma^2_{R}}\right\}, \quad (5)$$

where, $D_{XY,i,j} \equiv \sqrt{(X_{2,i}-X_{2,j})^2+(Y_{2,i}-Y_{2,j})}$, $D_{Z,i,j} \equiv Z_{2,i}-Z_{2,j}$, and $D_{R,i,j} \equiv R_{2,i}-R_{2,j}$. σ_{XY}, σ_Z and σ_R are constants, which are determined by the sensor interval.

C. Incorporation with RPM and DBIM

To reduce the unknown quantities processed in DBIM, the proposed method ncorporates the RPM based ROI determination into the DBIM method. First of all, the dielectric constant of background media is roughly estimated by the DBIM by assuming that a whole ROI area is homogeneous. Under this assumption, $\Delta O(\boldsymbol{r})$ becomes a constant ΔO_c, then Eq. (3) is reformulated as:

$$\Delta E^t(\boldsymbol{r},\omega) \simeq \omega^2\mu\Delta O_c \int_\Omega G_b(\boldsymbol{r}',\boldsymbol{r},\omega)E^t_b(\boldsymbol{r}',\omega)d\boldsymbol{r}'. \quad (6)$$

Since the number of unknown is only one pair of real and imaginary part of the object function of ΔO_c, the problem

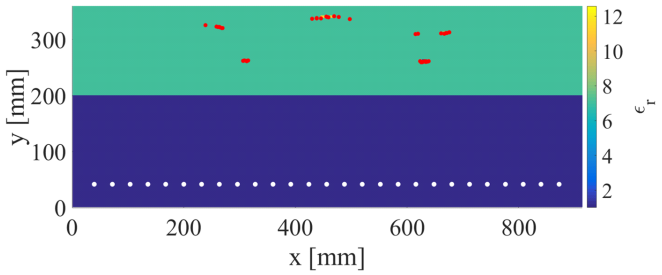

Fig. 4: Scattering center points (red solid circles) estimated by the RPM method.

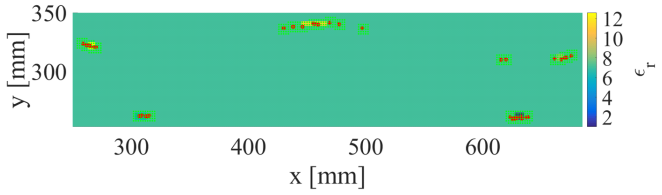

Fig. 5: ROI area (green dots) limited by the RPM imaging points (red solid circles).

becomes well-posed and an average dielectric property of the background media would be accurately determined.

TABLE I: Dielectric properties and size of background medium and each target.

	ϵ_r	σ [S/m]	size [mm]
Background medium	7.0	0.001	1006×360
Black rust (#1)	12.58	1.31	6×6
Salt rust (#2)	5.33	0.29	10×6
Hydrated black rust (#3)	11.28	1.14	22×4
Air cavity (#4)	1	0	8×6
Red rust (#5)	8.42	0.57	6×6

Next, the RPM determines the target boundary using the above relative permittivity of background media. For each scanning center point, the small size of ROI is given as $\Omega_i^{\rm obj}$, where i denotes the index of scattering center. Finally, the DBIM reconstructs the dielectric profile, where Eq. (3) is reformulated as;

$$\Delta E^t(\boldsymbol{r},\omega) \simeq \omega^2\mu\Delta O_c \int_{\Omega_{bg}} G_b(\boldsymbol{r}',\boldsymbol{r},\omega)E^t_b(\boldsymbol{r}',\omega)d\boldsymbol{r}' + \omega^2\mu\sum_i \int_{\Omega_i^{\rm obj}} G_b(\boldsymbol{r}',\boldsymbol{r},\omega)E^t_b(\boldsymbol{r}',\omega)\Delta O(\boldsymbol{r}')d\boldsymbol{r}', \quad (7)$$

where Ω^{bg} denotes the ROI of background media except for those of objects as $\sum_i \Omega_i^{obj}$. Figure 2 shows the flowchart of the proposed method.

IV. Numerical Test

This section describes the numerical simulation for evaluating the methods, using the two-dimensional (2-D) FDTD method, assuming the NDT observation model. 27 set of

ISBN 978-90-827970-1-5 © EURASIP 2018

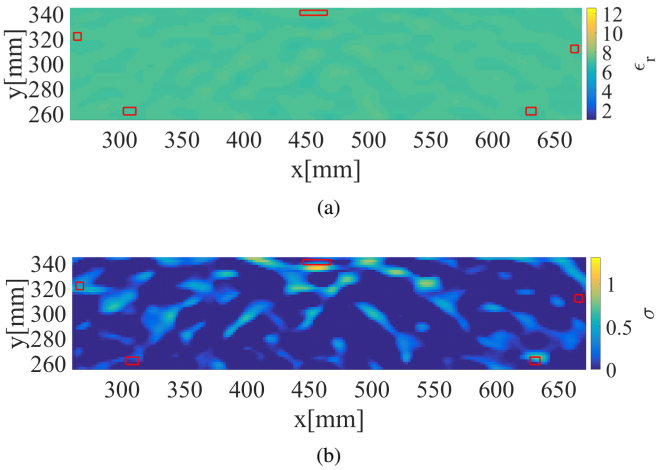

Fig. 6: Reconstructed dielectric map in case unknowns inside of whole area is processed. (a) Relative permittivity. (b) Conductivity.

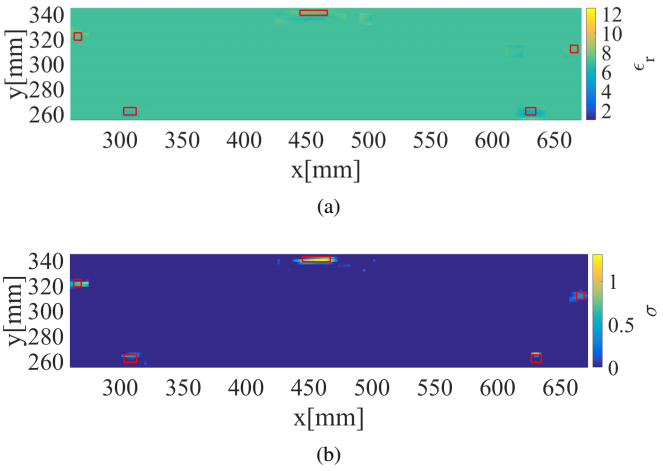

Fig. 7: Reconstructed dielectric map by the proposed algorithm.(a) Relative permittivity. (b) Conductivity.

transmitting and receiving antenna are linearly arranged with 30 mm equally spacing on the line , the distance to which is 158 mm from the surface of background media which includes five targets. The transmitted signal is Gaussian-modulated pulse with 2.45 GHz center frequency and 2.7 GHz bandwidth. Figure 3 indicates numerical simulation model. Five different types of target with small size are buried into concrete media, where each target size and its dielectric property is summarized on Table I, where the part of rust properties are referred from Qaddoumi *et al* [4]. The cell size for each unknown area is 2mm square, and the total number of unknowns in whole ROI is 40240. The initial DBIM for background media, based on Eq. (6), provides the rough estimation for relative permittivity as 7.1547 and the conductivity as 0.0021 S/m. Figure 4 demonstrates that the RPM method accurately determines the scattering center and is promising for the prior knowledge of ROI area.

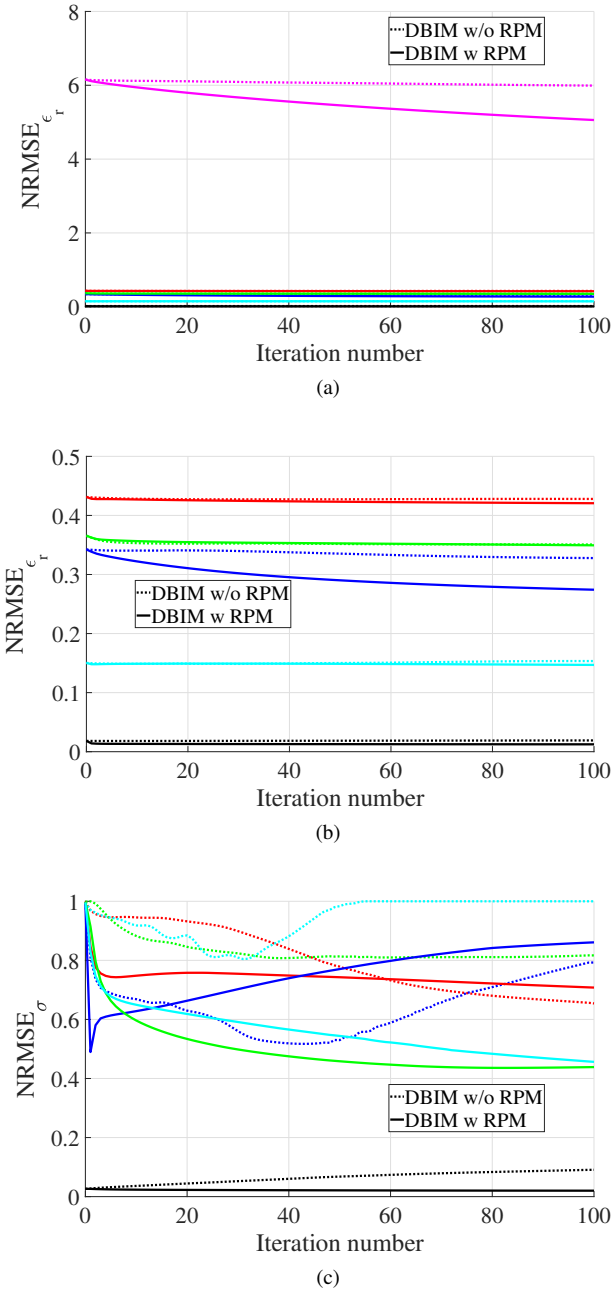

Fig. 8: NRMSEs for reconstruction. (a) Relative permittivity, (b) Relative permittivity (partial enlarged view), (c) Conductivity. (black: whole area, red: #1 target, blue: #2 target, green: #3 target, magenta: #4 target, cyan: #5 target)

Figure 5 shows estimated boundary points by RPM and the limited ROI area. Here, the ROI area for each scattering center is determined as the region spanned by 5×5 cells. Figures 6 and 7 show the dielectric maps reconstructed by the original DBIM method, where the whole ROI area is processed, and the proposed method. The number of unknowns for the original DBIM and the proposed method are 80480 and 960, respectively (98.8 % reduced). Figures 6 and 7 visually verify that our proposed method reconstructs

ISBN 978-90-827970-1-5 © EURASIP 2018

the actual dielectric property, compared with that obtained by the original method. The estimated background relative permittivity and the conductivity after 100 iteration 7.00 are 0.0012 S/m. For the quantitative analysis, the normalized root mean square error (NRMSE) for relative permittivity and conductivity for the i-th target area is given by:

$$\mathrm{NRMSE}_{\epsilon_r,i} = \frac{1}{\bar{\epsilon}_{r,i}} \sqrt{\frac{1}{K_i} \sum_{k=1}^{K_i} |\hat{\epsilon}_r(\boldsymbol{r}_k) - \epsilon_{r,\mathrm{true}}(\boldsymbol{r}_k)|^2}, \quad (8)$$

$$\mathrm{NRMSE}_{\sigma,i} = \frac{1}{\bar{\sigma}_i} \sqrt{\frac{1}{K_i} \sum_{k=1}^{K_i} |\hat{\sigma}(\boldsymbol{r}_k) - \sigma_{\mathrm{true}}(\boldsymbol{r}_k)|^2}, \quad (9)$$

where $\bar{\epsilon}_{r,i}$ and $\bar{\sigma}_i$ denote the maximum value of actual relative permittivity and conductivity for each target area. $\hat{\epsilon}_r$ and $\hat{\sigma}$ are estimated relative permittivity and conductivity, respectively. $\epsilon_{r,\mathrm{true}}$ and σ_{true} are true value of relative permittivity and conductivity, respectively. K_i is the total number of unknowns for the i-th ROI area. Figure 8 shows the each NRMSE for the relative permittivity and the electric conductivity for each target number. The results demonstrate that the proposed method improves the imaging accuracy of whole area and some targets. Any target case, the proposed method more rapidly reaches to minimal NRMSE, while a few cases show little deviation, *e.g.*, black rust or salt rust. We also confirm that the results largely depend on an initial dielectric property value, and it is next task to determine an appropriate initial value.

V. Conclusion

This paper proposed an efficient inverse scattering algorithm by incorporating RPM method into DBIM for microwave NDT observation model. In this method, the background dielectric constant is roughly estimated by the DBIM, where the number of unknowns are considerably reduced under homogeneous assumption. The ROI area is sequentially narrowed by the results from RPM imaging, and the DBIM is finally applied for the limited area to enhance the accuracy and convergence speed. The FDTD-based numerical test, assuming various type of dielectric object, *e.g.*, air cavity and various type of rust demonstrated that our proposed method considerably enhanced the accuracy even with less amount of observation data, compared with that obtained by tomographic model.

Acknowledgment

This research was supported by JST, PRESTO, Grant Number JPMJPR1771, Japan.

References

[1] T. Lasri and R. Zoughi, "Advances and applications in microwave and millimeter wave nondestructive evaluation," *Subsurface Sensing Technol. Applicat*., vol. 2, no. 4, Oct. 2001.

[2] M. Fallahpour, J.T. Case, M. Ghasr, and R. Zoughi, "Piecewise and wiener filter-based sar techniques for monostatic microwave imaging of layered structures", *IEEE Trans. Antennas Propaga*, vol. 62, no. 1, pp. 1-13, Jan. 2014

[3] M. Salucci, G. Oliveri, and A. Massa, "GPR Prospecting through an inverse scattering frequency-hopping multi-focusing approach," *IEEE Trans. Geosci. Remote Sens*., vol. 53, no. 12, pp. 65736592, Dec. 2015.

[4] R. Zoughi, *Microwave Nondestructive Testing and Evaluation*, The Netherlands: Kluwer Academic, 2000.

[5] W. C. Chew and Y. M. Wang, "Reconstruction of two-dimensional permittivity distribution using the distorted Born iterative method," *IEEE Trans. Med. Imag*., vol. 9, pp. 218225, June 1990.

[6] S. Kidera, T. Sakamoto, and T. Sato, "Accurate UWB Radar 3-D Imaging Algorithm for Complex Boundary without Range Point Connections," *IEEE Trans. Geosci. Remote Sens*., vol. 48., no. 4, pp. 1993-2004, Apr. (2010).

[7] K. Akune, S. Kidera, and T. Kirimoto "Accurate and Nonparametric Imaging Algorithm for Targets Buried in Dielectric Medium for UWB Radars," *IEICE Trans*. Electronics., vol. E95-C, No. 8, pp. 1389-139, Aug. 2012.

[8] T. Manaka, S. Kidera and T. Kirimoto, "Experimental study on embedded object imaging method with range point suppression of Creeping Wave for UWB radars", *IEICE Trans. Electron* Vol.E99-C,No.1,pp.138-142, Jan. 2016.